Microstructural Features of Prematurely Failed Hot-Strip Mill Work Rolls: Some Studies in Spalling Propensity

Amitava Ray, M.S. Prasad, S.K. Dhua, S.K. Sen, and S. Jha

(Submitted 21 October 1999; in revised form 28 March 2000)

Work rolls made of indefinite chill double-poured (ICDP) iron are commonly used in the finishing trains of hot-strip mills (HSMs). In actual service, spalling, apart from other surface degeneration modes, constitutes a major mechanism of premature roll failures. Although spalling can be a culmination of roll material quality and/or mill abuse, the microstructure of a broken roll can often unveil intrinsic inadequacies in roll material quality that possibly accentuate failure. This is particularly relevant in circumstances when rolls, despite operation under similar mill environment, exhibit variations in roll life.

The paper provides an insight into the microstructural characteristics of spalled ICDP HSM work rolls, which underwent failure under similar mill operating environment in an integrated steel plant under the Steel Authority of India Limited. Microstructural features influencing ICDP roll quality, viz. characteristics of graphite, carbides, martensite, etc., have been extensively studied through optical microscopy, quantitative image analysis (QIA), and electron-probe microanalysis (EPMA). These are discussed in the context of spalling propensity and roll life.

Keywords failure analysis, hardness, hot-strip mill, microstructure spalling

1. Introduction

In the finishing trains of hot-strip mills (HSMs), work rolls made of indefinite chill double-poured (ICDP) iron are commonly used owing to their resistance to wear and thermal fatigue.[1] These ICDP rolls are characterized by a "shell" (or chill) of alloy cast iron and a softer core of gray/nodular iron. During service, these rolls may fail prematurely owing to improper mill operating environment and/or inadequacies in roll material quality. The problem of such failures is relatively more acute in modern high-performance HSMs, where work rolls are subjected to higher mechanical stresses owing to demands of mill productivity and superior product quality.[2] Work rolls used in the finishing stands of HSMs may suffer from surface degeneration and banding, firecracking, surface indentation, and spalling.[3] While roll surface deterioration by the first three phenomena are progressive in nature and can be remedied from time-to-time by roll grinding operations, this nevertheless reduces the working diameter and in turn the useful roll life. Spalling, on the other hand, can culminate in catastrophic roll failures leading to considerable reduction in roll life and mill productivity.

Spalling involves a fatigue phenomenon, where fracture occurs by generation and propagation of several microcracks under applied stresses imposed during rolling. Although spalling is often a consequence of mill-related factors,[4] the influence of roll material quality in inducing such failure is by no means insignificant. This is particularly relevant in circumstances when rolls, despite operation under similar mill environment, exhibit variations in roll life.[5] In such instances, the microstructure of a failed roll can often provide insight into intrinsic quality deficiencies that possibly accentuate premature spalling. It is in this perspective that an extensive microstructural investigation has been carried out on spalled samples of ICDP work rolls used in the finishing stands of a HSM. The study pertains to an integrated steel plant under the Steel Authority of India Limited, where large variations in HSM work roll life were observed even under similar mill operating environment.

The paper discusses microstructural aspects such as graphite morphology and content, carbide characteristics, and nature of the martensite matrix in spalled ICDP HSM work rolls in the context of spalling propensity and roll life.

2. Experimental

Spalled samples were collected from the barrel portion of prematurely failed HSM work rolls, which gave varying roll lives under similar mill operating environment. The fragmented samples of spalled rolls were cleaned with acetone and examined with respect to their visual appearance, fracture features, and microstructural characteristics.

For optical microscopy, specimens of around 25 × 10 × 15 mm dimensions were cut along the radial cross sections of spalled rolls. These specimens were ground and polished to a scratch-free finish for metallographic observation. Polished and unetched specimens were examined by optical microscopy at magnifications of 500× and 100× to observe the graphite morphology and distribution, respectively. The unetched roll specimens were also observed for non-metallic inclusions (NMI) at 500× magnification. Microstructural examinations were also carried out on natal-etched specimens (2 mL concentrated HNO_3 in 98 mL ethyl alcohol) of failed rolls to observe

Amitava Ray, M.S. Prasad, S.K. Dhua, S.K. Sen, and S. Jha, Physical Metallurgy Group, Research and Development Centre for Iron and Steel, Steel Authority of India Limited, Ranchi-834002, India.

characteristics of matrix phases such as martensite, retained austenite, and carbides. Microhardness [Vickers pyramid number (VPN)] measurements were concurrently carried out on different phases to corroborate their identity. For determining the microhardness of hard martensite and carbide phases, a 50 g indenting load was applied, while a lower load of 10 g was used for the softer graphite phase.

Quantitative image analysis (QIA) was carried out in a "Quantimet-600" (LEICA Imaging Systems Ltd., Cambridge, United Kingdom) model equipment to determine the volume fractions of different phases present in the failed roll samples. The volume fractions of graphite were determined from polished and unetched specimens, while nital-etched specimens were used for estimating the contents of other microstructural constituents such as martensite, retained austenite, and carbide. In estimating the volume fractions of carbide and retained austenite, thresholding and image editing were performed selectively since both these phases appeared white under bright-field microscope illumination. Initially, thresholding was done by selecting a video level to capture both the carbide and retained austenite phases, and the overall volume fraction (*i.e.*, carbide plus retained austenite) was determined for a particular microscopic field. Subsequently, the carbide phase in the same field was selectively delineated by binary image editing and its volume fraction determined. The difference in the values of the aforesaid two volume fraction measurements gave the volume fraction of retained austenite. Since ICDP rolls primarily consist of four microstructural constituents (graphite, carbide, martensite, and retained austenite), the volume fraction of martensite in a particular field was empirically determined by subtracting the total volume fractions of graphite, carbide, and retained austenite from 100%. For ensuring measurement authenticity and accuracy, QIA was carried out over a large number (at least 50) of microscopic fields at 200× magnification to determine the average volume fractions of various microstructural constituents.

Fractographic observations of failed roll samples were carried out at 1000× magnification in a "JSM-840A" (JEOL Ltd., Akishima, Tokyo) model scanning electron microscope (SEM) to study the general surface topography and features associated with the failure. In parallel, electron-probe microanalysis (EPMA) was carried out in a "JCXA-733" (JEOL Ltd.) model EPMA, on polished and unetched roll specimens to identify elements present in the graphite phase and matrix regions, as well as to characterize non-metallic impurity. The EPMA investigations were also carried out on nital-etched roll specimens to determine elemental enrichment in the carbide phase. Qualitative and quantitative analyses of carbides were carried out by using JEOL proprietary "QLAN" and "PACM" application software, respectively, under 15 kV accelerating voltage and 5×10^{-8} A probe current.

3. Results and Discussion

3.1 Roll Particulars

The ICDP work rolls used in the finishing stands of this particular HSM are of 810 mm barrel diameter (nominal) and 2000 mm barrel length. The hardness on the working surface of new rolls ranges between 80 and 85° shore "C." The normal chemistry (in wt.%) of the "shell" material in such ICDP rolls is 3.30 to 3.40 C; 0.75 to 0.95 Mn; 0.85 to 1.00Si; 4.10 to 4.30Ni; 1.50 to 1.95Cr, and 0.30 to 0.40Mo. The rolls are commissioned in the mill at their initial diameter of 810 mm and are scrapped in normal usage when the working diameter wears down and reaches 750 mm. This means that the shell region in these ICDP work rolls is around 30 mm [(810 to 750 mm)/2] on the radius.

Table 1 Roll particulars and life data

Roll sample	Supplier	Roll diameter at spalling stage (mm)	Roll life (tonnes)	Average roll life (tonnes)
HSM #1	A	808.35	6,142	
HSM #2	A	803.00	25,224	
HSM #3	B	801.90	38,045	
HSM #4	C	800.85	42,869	
HSM #5	B	796.50	54,268	48,387.22
HSM #6	A	780.75	63,513	
HSM #7	C	793.35	63,786	
HSM #8	B	750.20	69,328	
HSM #9	C	791.95	72,310	
HSM #10	C	749.10	113,173	
HSM #11	B	783.50	113,843	
HSM #12	D	750.80	137,001	
HSM #13	C	750.35	146,664	146,101.71
HSM #14	C	773.75	157,615	
HSM #15	B	750.20	171,730	
HSM #16	A	750.60	182,686	

The details of the spalled HSM work rolls investigated with regard to their identification number, roll life (*i.e.,* tonnage rolled prior to failure), and roll diameter at spalling stage are shown in Table 1. It is clearly evident from this table that out of the 16 roll samples investigated, 10 samples (HSMs #1, 2, 3, 4, 5, 6, 7, 9, 11, and 14) pertained to the working surface of rolls that spalled at higher diameter (773 to 808 mm), *i.e.*, possibly from the shell regions of these rolls. On the contrary, the other six roll samples (HSMs #8, 10, 12, 13, 15, and 16) were virtually obtained at the scrap diameter (749/750 mm) stage, *i.e.,* almost at the initiation of the roll "core" region.

The roll lives depicted in the aforesaid table were found to vary widely and ranged between 6142 to 182,686 tonnes. It is expedient to mention that roll life in steel mills is customarily indicated in terms of tonnage of material rolled (i.e., cumulative quantity of rolled material produced in several campaigns prior to discard/failure of a given roll) rather than hours of operation. This is because time related data often involves breakdown/maintenance activities, whereas mill production data (i.e., tonnage rolled) is more authentic.

In the first nine rolls (HSMs #1 to 9), the lives varied between 6142 and 72,310 tonnes, with an average value of 48,387 tonnes, whereas in the subsequent seven rolls (HSMs #10 to 16), the lives ranged between 113,173 and 182,686 tonnes, with an average value of 146,101 tonnes. It can thus be seen that the average life obtained in the latter seven rolls (HSMs #10 to 16) was almost three times the average life obtained in the first nine rolls (HSMs #1 to 9). Table 1 also reveals that of the 16 rolls investigated, 25% of rolls exhibited lives less than 50,000 tonnes, 31.25% of rolls between 50,000 and 75,000 tonnes, and 43.75% of rolls greater than 100,000 tonnes.

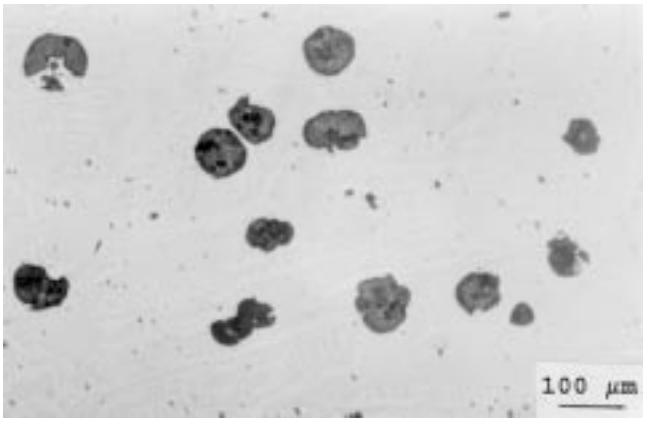

Fig. 1 Optical micrograph showing mostly nodular graphite morphology in the shell region of roll sample HSM #14; magnification 100×

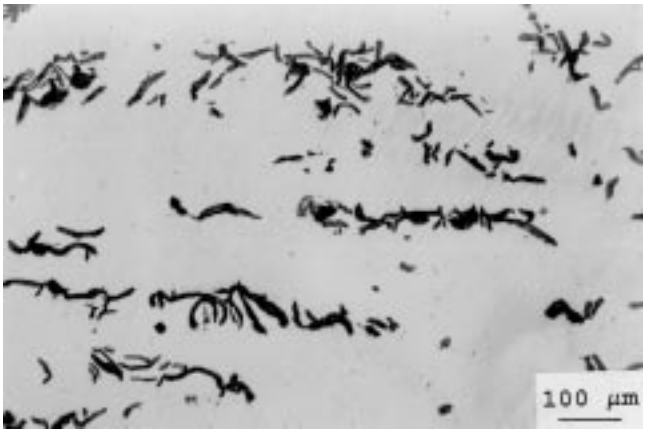

Fig. 2 Optical micrograph showing typical flake graphite morphology in the shell region of roll sample HSM #4; magnification 100×

3.2 Microstructural Features

Graphite Characteristics. Out of ten spalled samples pertaining to the shell region (*i.e.*, where the diameter at spalling was >750 mm), nodular graphite morphology was observed in the optical microstructures of four roll samples: HSMs #7, 9, 11, and 14, which gave an average roll life of 101,888 tonnes. These four rolls exhibited comparatively higher average roll lives than the other six rolls: HSMs #1 to 6 (average roll life = 38,343 tonnes) showed flake graphite. Typical optical micrographs showing nodular and flake graphite morphologies in roll samples HSM #14 (life = 157,615 tonnes) and HSM #4 (life = 42,869 tonnes) are shown in Fig. 1 and 2, respectively, at 100× magnification.

The graphite morphologies of the other six roll samples (HSMs #8, 10, 12, 13, 15, and 16), which also spalled at the scrap diameter stage, were flaky. This is expected since the core structure of ICDP rolls usually consists of flake-like graphite.[6] Thus, in this case, the role of graphite morphology in influencing roll life cannot be opined. The graphite morphology in roll sample HSM #16, which gave the highest roll life (182,686 tonnes), was partly nodular and partly flaky. Although this particular sample was obtained at a scrap diameter of 750.60 mm, the coexistence of both nodular and flake graphite morphologies at the scrap diameter stage is indicative of a shell-core transition zone. It can therefore be inferred that the graphite morphology in the shell region of roll HSM #16 was nodular.

Fig. 3 Nital-etched microstructure of roll HSM #8 showing acicular martensite with retained austenite at needle interstices and white carbide phase exhibiting microcracking; magnification 500×

The favorable effect of nodular graphite morphology in the shell microstructure toward enhancing roll life is thus evident from the above studies. This finding is corroborated by the fact[7] that spheroidal irons by virtue of their lower thermal conductivity, higher elastic modulus, and greater tensile strength than flake irons are more crack resistant under conditions of higher induced thermal stresses. However, crack generation was possible even in spheroidal irons under very high thermal stresses owing to its insufficient yield and creep resistance. This could have possibly happened in HSMs #7 and 9, which, despite having nodular graphite morphology, failed to perform to the desirable extent. Horvath,[8] in his studies on the relationship between roll surface breakdown and scale formation, has clearly mentioned the importance of graphite morphology in influencing crack initiation. In his studies on ICDP rolls, it was observed that flake graphite acted as a potential stress raiser, leading to the initiation of microcracking in rolls. In contrast, spheroidal graphite particles did not act as stress raisers and, hence, were less susceptible to thermal fatigue cracking and removal from the roll surface.

Matrix Characteristics. The nital-etched microstructures of all failed roll samples showed martensite (dark gray to black) with retained austenite in needle interstices, carbide (white), and graphite phases. The carbide phase was of eutectic type and appeared in continuous networks. Typical micrographs of nital-etched roll specimens HSMs #8, 14, and 1 are shown in Fig. 3, 4, and 5, respectively, at 500× magnification. It is clearly seen from these micrographs that, although microstructural constituents (martensite, retained austenite, and carbide) are essentially the same in all three roll samples, microstructural degeneration is manifested as microcracking in the carbide phase and could only be observed in roll samples HSM #8 (life = 69,328 tonnes) and HSM #1 (life = 6142 tonnes). The microcracks in the carbide phase might possibly have generated during rolling and propagated under applied stresses to ultimately result in premature spalling. It has been reported[9] that

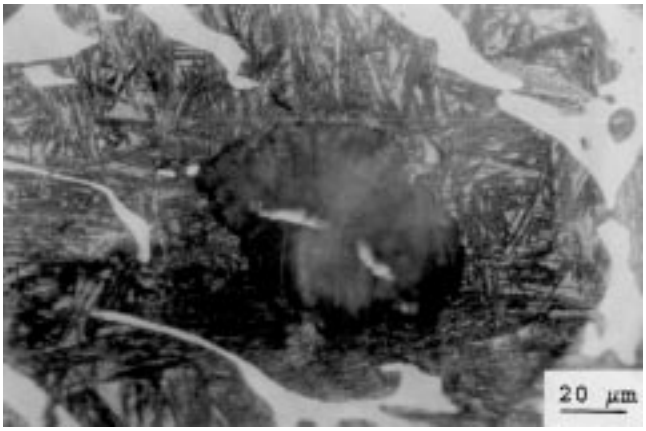

Fig. 4 Nital-etched microstructure of roll HSM #14 showing acicular martensite with retained austenite at needle interstices, white carbide phase, and dark-gray graphite nodule; magnification 500×

Fig. 5 Nital-etched microstructure of roll HSM #1 showing acicular martensite with retained austenite at needle interstices and white carbide phase exhibiting pronounced microcracking; magnification 500×

cracks may occur in large eutectic carbides concomitantly with thermal fatigue cracks that form on the roll surface. The cause of such cracking of carbides has been attributed to thermal reasons or, more likely, could be mechanically induced by work roll/backup roll contact stresses, or by rolling stresses. The microhardness values of martensite, carbide, and graphite phases were determined for all of the failed roll samples and are shown in Table 2. It can be seen that, while the microhardness of martensite ranged from 541 to 644 VPN, that of the carbide phase varied between 1000 and 1345 VPN. The microhardness of graphite, however, was found to be consistent and ranged between 50 to 54 VPN in all of the spalled roll samples.

The data in Table 2 reveal that the carbide microhardness of the first nine rolls (HSMs #1 to 9) ranged between 1100 and 1345 VPN, with an average value of 1157.77 VPN. On the other hand, carbide microhardness in the other seven rolls (HSMs #10 to 16), which gave significantly higher roll lives ranging between 1000 and 1095 VPN, with an average value of 1058.86 VPN. It is thus evident that carbide microhardness in the latter group of seven higher life rolls (average roll life = 146,101 tonnes) was about 100 VPN lower than the former group of nine lower life (average roll life = 48,387 tonnes) rolls.

Table 2 Microhardness values of different phases in HSM work roll samples

	Average microhardness (VPN)		
Roll sample	**Martensite**	**Carbide**	**Graphite**
HSM #1	644	1345	50
HSM #2	615	1150	54
HSM #3	633	1180	53
HSM #4	603	1120	54
HSM #5	595	1200	52
HSM #6	603	1100	54
HSM #7	603	1120	53
HSM #8	585	1105	52
HSM #9	598	1100	53
HSM #10	562	1050	52
HSM #11	585	1095	51
HSM #12	541	1000	51
HSM #13	562	1050	54
HSM #14	566	1095	51
HSM #15	567	1072	54
HSM #16	566	1050	51

It can also be seen from Fig. 3 to 5 that the amount of microcracking is particularly pronounced in roll sample HSM #1 (roll life = 6142 tonnes), which incidentally exhibited a very high microhardness (1345 VPN) of the carbide phase. A close examination of the roll life data (Table 1) and the carbide microhardness values (Table 2) shows the vulnerability of rolls exhibiting carbide microhardness higher than 1100 VPN. This condition could possibly enhance microcracking propensity and, hence, lead to subsequent spalling of rolls.

3.3 Volume Fractions of Microstructural Phases

The volume fractions (in %) of constituent microstructural phases in the spalled roll samples were determined by OIA. The image analysis data pertaining to average volume fractions of graphite, carbide, martensite, and retained austenite are shown in Table 3. The volume fraction of martensite was found to range between 42.09 and 61.25%, carbide phase between 20.60 and 43.05%, retained austenite between 5.86 and 16.32%, and graphite between 2.51 and 5.18%. It is interesting to observe that the graphite volume fraction (Table 3) in nine rolls (HSMs #1 to 9), which exhibited lower roll lives (i.e., 6142 to 72,310 tonnes; average: 48,387 tonnes), varied from 2.51 to 4.49%, with an average value of 3.38%. In contrast, the other seven rolls (HSMs #10 to 16), which exhibited superior roll lives (*i.e.*, 113,173 to 182,686 tonnes; average: 146,101 tonnes), showed higher graphite volume fractions, ranging between 4.05 and 5.18%, with an average value of 4.44%. It is apparent from the aforesaid observations that, while graphite volume fractions in the range of 4 to 5% are conducive to better roll life, a lower volume fraction (<4%) is deleterious. As a matter of fact, six rolls (HSMs #1, 2, 3, 5, 7, and 8), which had particularly low roll lives, showed graphite volume fractions in the range of 2.51 to 3.54%.

Iron carbide that can comprise up to 40% by area of the roll microstructure has a profound effect on the properties and mill performance of iron rolls.[10] Investigators[11] have reported

Table 3 QIA data showing volume fractions of different phases in spalled roll samples

	Volume fraction (%)			
Roll sample	Martensite	Carbide	Retained austenite	Graphite
HSM #1	46.57	38.99	11.82	2.62
HSM #2	49.80	37.17	9.49	3.54
HSM #3	46.16	37.86	13.12	2.86
HSM #4	53.99	34.53	6.99	4.49
HSM #5	48.46	43.05	5.86	2.63
HSM #6	52.40	34.68	8.90	4.02
HSM #7	42.09	38.82	15.92	3.17
HSM #8	52.91	33.14	11.44	2.51
HSM #9	50.68	34.15	10.56	4.61
HSM #10	60.14	20.60	14.37	4.89
HSM #11	58.35	30.08	7.52	4.05
HSM #12	51.94	27.36	16.32	4.38
HSM #13	56.35	22.71	15.76	5.18
HSM #14	58.41	22.63	14.56	4.40
HSM #15	61.25	21.80	12.80	4.15
HSM #16	54.45	30.20	11.32	4.03

that pitting commonly observed in the last three stands of HSMs is associated with loss of mass from the roll surface. This phenomenon is aggravated as large primary dendritic carbides stand out without any mass support and fragment or come out completely from the martensitic matrix. Table 3 shows that the volume fraction of martensite ranged between 42.09 and 53.99% (average: 49.23%) in the nine roll samples (HSMs #1 to 9), which exhibited lower average (48,387 T) lives. In contrast, martensite volume fraction was found to be higher (range: 51.94 to 61.25%; average: 57.27%) in the seven roll samples (HSMs #10 to 16), which showed superior lives It is therefore evident that the lower volume fraction of martensite (average: 49.23%) in the nine low life roll samples (HSMs #1 to 9) offered less matrix support area to hard carbides than that in the seven superior life rolls (HSMs #10 to 16), where average volume fraction (57.27%) of martensite was higher. The fragmentation of carbides, therefore, might have been presumably aided by less matrix (martensite) support area in lower life rolls.

The volume fraction of retained austenite was found to vary between 5.86 and 15.92% (average: 10.45%) in the low life roll samples (HSMs #1 to 9) and between 7.52 and 16.32% (average: 13.23%) in the seven higher life roll samples (HSMs #10 to 16). In this case, however, no clear relationship between volume fraction retained austenite and roll life was observed.

The carbide volume fractions in nine samples (HSMs #1 to 9), which gave lower roll lives, were found to vary between 33.14 and 43.05%, with an average value of 36.93%. In contrast, the carbide volume fractions in the other seven rolls, which gave relatively higher lives (HSMs #10 to 16), ranged between 20.60 and 30.20%, with an average value of 25.05%. It can therefore be seen that while a carbide volume fraction in the range of 20 to 30% is conducive to higher roll life, a higher carbide volume fraction (in the range of 35 to 45%) is deleterious. There is therefore a critical limit of carbide volume fraction, which can adversely influence the performance, and life of HSM work rolls. These findings are also corroborated by Lecomte-Mertens,[12] who observed that roll hardness was a direct function of carbide content and that carbides play an important role in the cracking process. According to Hertz theory, stress concentrations are located 3 or 4 mm below the surface of rolls. Additional stress concentrations arise from interaction between the more ductile matrix and the harder carbides, giving rise to the splitting of the matrix-carbide interface or breakage of the carbides, which are prone to fracture, due to low tensile strength. Once cracks appear in the broken carbides or along them, they propagate and join together in a pattern that leads to spalling. In ICDP rolls, the carbide phase is characteristically continuous and, hence, the propagation of cracks is more rapid along carbides. It is thus expedient to mention that, although higher carbide volume fractions enhance hardness, abrasion, and wear resistance, they nonetheless increase the propensity to cracking.

3.4 Fracture Characteristics

The SEM examinations were carried out at both low and high magnifications to obtain a general image of the fracture topography as well as for observing surface features in greater detail. The general fracture topography of all spalled rolls showed brittle features. Figure 6(a) shows the SEM photograph of the fracture surface of roll sample HSM #9 at 1000× magnification. The fracture topography is brittle and shows the decohesion of a graphite nodule. The fracture surface of the same sample at another region is also shown in Fig. 6(b) at 1000× magnification. It is evident from Fig. 6(a) that, although the fracture topography is essentially brittle, it is also associated with localized ductile regions (dimpled appearance) in the vicinity of the graphite nodule. The fracture features observed in Fig. 6(b) are, however, primarily brittle (cleavage) and show manifestations of intergranular cracking and cleavage steps.

3.5 EPMA of Phases and Inclusions

The EPMA of nodular graphite particles in roll samples HSMs #7, 9, 11, 14, and 16 revealed the presence of Al, Si, Mg, and Ca in addition to C, while graphite flakes in the other 11 spalled roll samples did not show the presence of Mg. This clearly indicated that magnesium was used as an inoculant for the manufacture of rolls exhibiting nodular iron in the 'shell' regions. The matrix regions in all the spalled roll samples, however, showed the presence of Fe, Si, Ni, and Cr. The backscattered electron (BSE) image of typical nodular graphite particles observed in roll sample HSM #9 is shown in Fig. 7(a) at 180×. The corresponding x-ray dot-mapping images of C, Si, Cr, and Ni are shown in Fig. 7(b), (c), (d), and (e), respectively.

The EPMA investigations of typical NMIs present in the spalled HSM roll samples revealed the existence of both TiN- and MnS-type inclusions. The BSE and x-ray dot mapping images of a typical TiN associated MnS inclusion found in roll sample HSM #3 (roll life = 38,045 tonnes) are shown in Fig. 8(a) to (d) at 1000× magnification. It is expedient to mention that, although MnS inclusions were observed in many roll specimens, rolls exhibiting lower roll life were found to show a higher incidence of brittle and angular TiN inclusions.

Quantitative EPMA was carried out to determine the chemistry and also to ascertain the type of carbides present in the spalled HSM roll samples. For analytical authenticity, a number of carbides in each spalled roll sample were analyzed. Table 4 shows the ZAF (Z: atomic number correction factor; A: absorption correction factor; F: fluorescence correction factor) corrected quantitative EPMA data of typical eutectic-type carbides

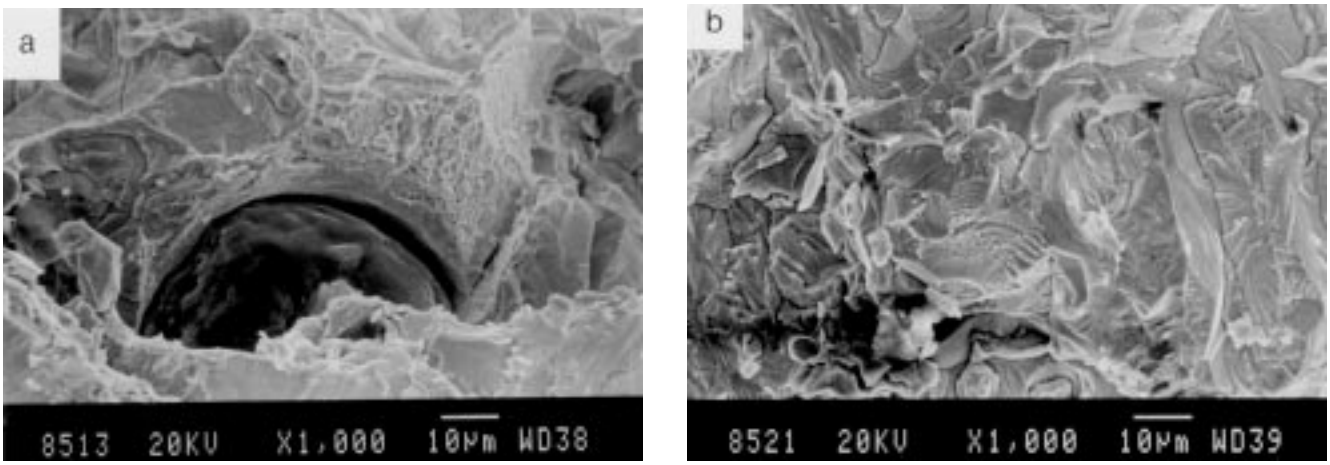

Fig. 6 SEM fractographs of roll sample HSM #9 showing (**a**) brittle features and small ductile zone as well as decohesion near graphite nodule and (**b**) essentially brittle area exhibiting intergranular cracking and cleavage steps; magnification 1000×

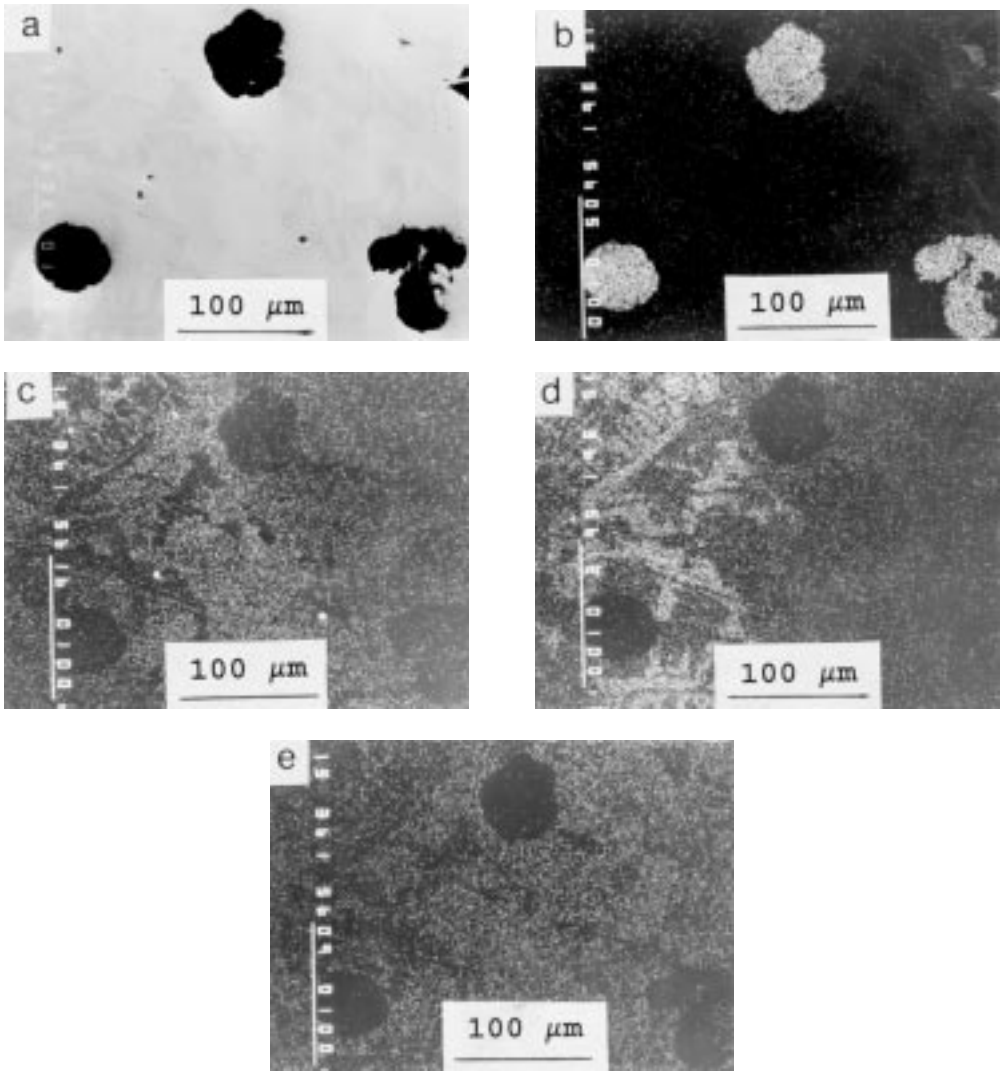

Fig. 7 EPMA scans of nodular graphite particles in roll sample HSM #9 showing (**a**) BSE image, (**b**) C x-ray map, (**c**) Si x-ray map, (**d**) Cr x-ray map, and (**e**) Ni x-ray map; magnification 180×

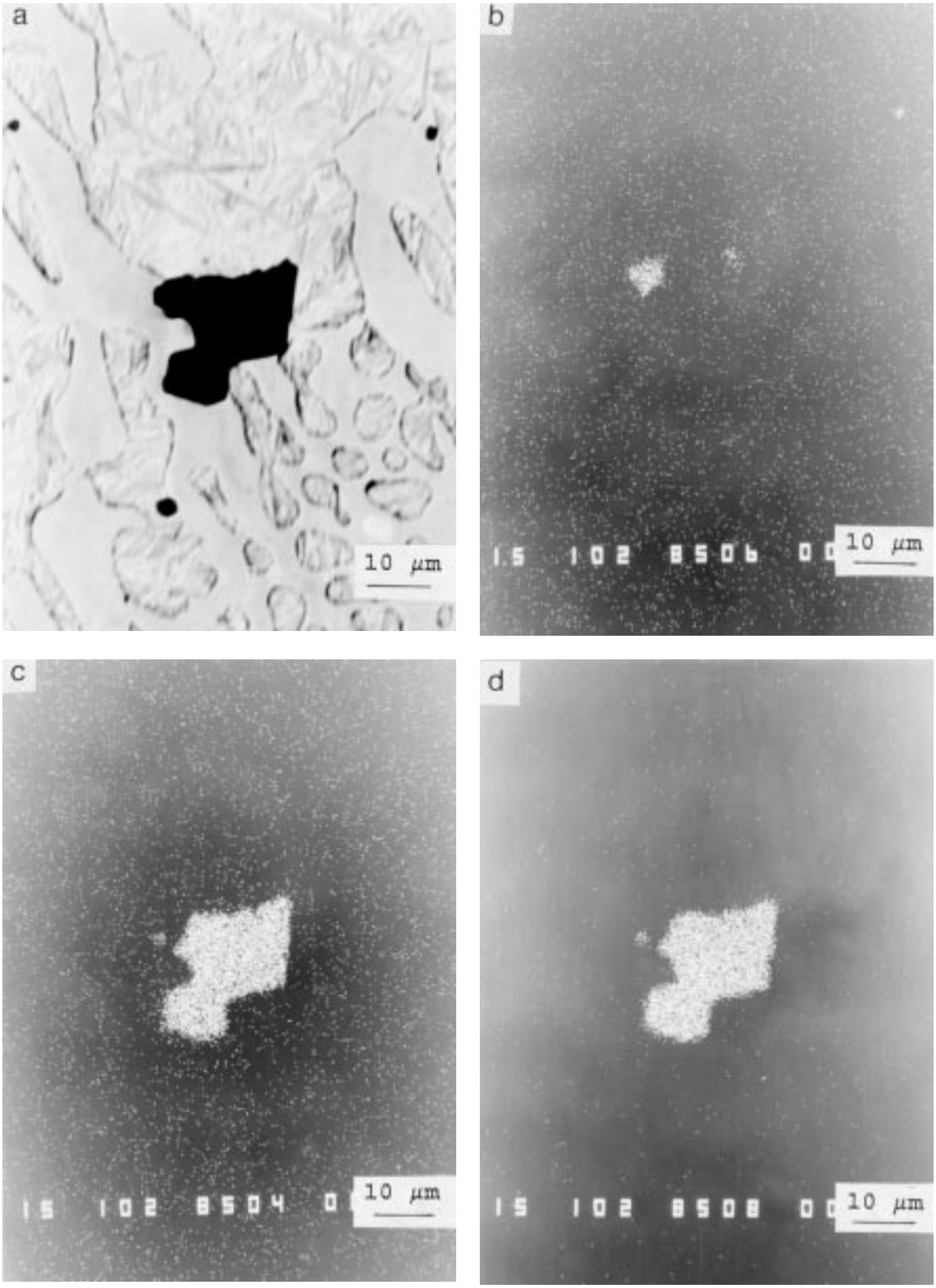

Fig. 8 EPMA scans of TiN associated sulfide inclusion in roll sample HSM #3 showing (**a**) BSE image, (**b**) Ti x-ray map, (**c**) Mn x-ray map, and (**d**) S x-ray map; magnification 1000×

Table 4 ZAF-corrected quantitative EPMA analysis of a typical M_3C-type eutectic alloy carbide in roll sample HSM #16

Element	Concentration (wt.%)	Concentration (at.%)	*K*(%)	ZAF	Z	A	F
C	7.853	27.912	2.956	2.6566	0.8264	3.2146	1.0000
Cr	4.669	3.833	5.613	0.8318	1.0213	1.0046	0.8107
Mn	1.149	0.893	1.104	1.0410	1.0398	1.0012	1.0000
Fe	88.018	67.273	85.959	1.0240	1.0203	1.0035	1.0000
Mo	0.201	0.089	0.163	1.2279	1.1092	1.1087	0.9985
	101.890	100.00	95.796	(PAC1)	(PH-TX)		

K: intensity ratio of a particular element in unknown sample and a pure standard
ZAF: atomic number, absorption, and fluorescence correction factor
Z: atomic number correction factor
A: absorption correction factor
F: fluorescence correction factor
PH-TX: Philibert-Tixier's formula for atomic number correction
PACI: file name for JEOL's quantitative analysis program for metals

observed in roll sample HSM #16. It can be seen from the aforesaid table that the carbon content of the carbide phase is 7.853 wt.%. The carbide essentially contains Fe (88.018 wt.%) and Cr (4.669 wt.%), with little amounts of Mn (1.149 wt.%) and Mo (0.201 wt.%). The atom percentage of carbon in this carbide is 27.912%, while the combined atom percentage of the other associated elements (*i.e.*, summation of Fe, Mn, Cr, and Mo) in the carbide was found to be 72.088%. This implies that the carbide phase in the spalled roll samples was essentially of M_3C type.

4. Conclusions

The following conclusions have emerged from the present study.

- Longer roll life is associated with a nodular graphite morphology in the shell (outer) portion of a roller; also, a graphite volume fraction 4 to 5% appears optimal.
- Among the different types of microstructural constituents observed in ICDP iron work rolls, the characteristics of the carbide phase have been found to exert a profound influence on roll spalling.
- Microstructural examination of low life rolls revealed pronounced microcracking of carbides. The tendency of such microcracking was particularly noticeable in higher hardness (>1100 VPN) carbides.
- OIA revealed that higher life rolls exhibited lower carbide volume fractions (range: 20.60 to 30.20%; average: 25.05%) than lower life rolls, where the carbide volume fraction (range: 33.14 to 43.05%; average: 36.93%) was higher. Thus, although carbides are indispensable for hardness, abrasion, and wear resistance of ICDP iron work rolls, a higher carbide volume fraction may enhance fragmentation and microcracking propensity and, in turn, accentuate subsequent spalling.

Acknowledgments

The authors are grateful to Dr. S.K. Bhattacharyya, Director, R&D Centre for Iron and Steel, SAIL (Ranchi), for his encouragement and support in pursuing this study. The excellent service rendered by the metallography laboratory personnel of RDCIS, especially Messrs. U.N. Jha, B.B. Patra, C.B. Sharma, and John Guria, during the entire course of the investigation merits special mention. The authors also record their appreciation for Mr. B. Khalkho for neatly typing the manuscript.

References

1. R.N. Shaughnessy: *J. Iron Steel Inst.*, 1968, vol. 206 (10), pp. 981-86.
2. B.M. Kapadia and K.W. Marsden: *37th Mechanical Working and Steel Processing Conf. Proc.*, Iron and Steel Society, Warrendale, PA, 1996, vol. 33, pp. 221-42.
3. M. Grounes and K. Inestam: *Iron Steel Eng.*, 1979, vol. 56 (4), pp. 42-49.
4. N.C. Nelson and C.O. Zamuner: *34th Mechanical Working and Steel Processing Conf. Proc.*, Iron and Steel Society, Warrendale, PA, 1993, vol. 30, pp. 205-09.
5. A. Ray, D. Mukherjee, B. Sarkar, and S. Mishra: *J. Mater. Eng. Performance*, 1994, vol. 3 (5), pp. 649-56.
6. B. Carmona, D.J. Tarney, and D.K. Tice: *33rd Mechanical Working and Steel Processing Conf. Proc.*, Iron and Steel Society, Warrendale, PA, 1992, vol. 29, pp. 193-205.
7. R. Elliott: *Cast Iron Technology*, Butterworth and Co. Ltd., London, 1988, p. 25.
8. P.J. Horvath: *22nd Mechanical Working and Steel Processing Conf. Proc.*, Iron and Steel Society, Warrendale, PA, 1980, vol. 18, pp. 238-49.
9. R.R. Judd: *Iron Steel Eng.*, 1979, vol. 56 (1), pp. 51-60.
10. W.H. Betts: *22nd Mechanical Working and Steel Processing Conf. Proc.*, Iron and Steel Society, Warrendale, PA, 1980, vol. 18, pp. 364-74.
11. M. Villanueva, L.A. Leduc, and G. Olvera: *34th Mechanical Working and Steel Processing Conf. Proc.*, Iron and Steel Society, Warrendale, PA, 1993, vol. 30, pp. 161-70.
12. C. Lecomte-Mertens: *33rd Mechanical Working and Steel Processing Conf. Proc.*, Iron and Steel Society, Warrendale, PA, 1992, vol. 29, pp. 119-28.